







# Left Prefrontal Connectivity Links Subthalamic Stimulation with Depressive Symptoms

Friederike Irmen, PhD <sup>1,2,3†</sup> Andreas Horn, MD, PhD <sup>1†</sup> Philip Mosley, PhD <sup>4,5</sup>  
Alistair Perry, PhD <sup>6,7</sup> Jan Niklas Petry-Schmelzer, MD <sup>8</sup> Haidar S. Dafsari, MD,<sup>8</sup>  
Michael Barbe, MD,<sup>8</sup> Veerle Visser-Vandewalle, MD,<sup>9</sup> Gerd-Helge Schneider, MD,<sup>10</sup>  
Ningfei Li, MSc <sup>1</sup> Dorothee Kübler, MD,<sup>1</sup> Gregor Wenzel, MD,<sup>1</sup> and  
Andrea A. Kühn, MD<sup>1,2,11</sup>

**Objective:** Subthalamic nucleus deep brain stimulation (STN-DBS) in Parkinson's disease (PD) not only stimulates focal target structures but also affects distributed brain networks. The impact this network modulation has on non-motor DBS effects is not well-characterized. By focusing on the affective domain, we systematically investigate the impact of electrode placement and associated structural connectivity on changes in depressive symptoms following STN-DBS, which have been reported to improve, worsen, or remain unchanged.

**Methods:** Depressive symptoms before and after STN-DBS surgery were documented in 116 patients with PD from 3 DBS centers (Berlin, Queensland, and Cologne). Based on individual electrode reconstructions, the volumes of tissue activated (VTAs) were estimated and combined with normative connectome data to identify structural connections passing through VTAs. Berlin and Queensland cohorts formed a training and cross-validation dataset used to identify structural connectivity explaining change in depressive symptoms. The Cologne data served as the test-set for which depressive symptom change was predicted.

**Results:** Structural connectivity was linked to depressive symptom change under STN-DBS. An optimal connectivity map trained on the Berlin cohort could predict changes in depressive symptoms in Queensland patients and vice versa. Furthermore, the joint training-set map predicted changes in depressive symptoms in the independent test-set. Worsening of depressive symptoms was associated with left prefrontal connectivity.

**Interpretation:** Fibers connecting the electrode with left prefrontal areas were associated with worsening of depressive symptoms. Our results suggest that for the left STN-DBS lead, placement impacting fibers to left prefrontal areas should be avoided to maximize improvement of depressive symptoms.

ANN NEUROL 2020;;87:962–975

View this article online at [wileyonlinelibrary.com](https://onlinelibrary.wiley.com/doi/10.1002/ana.25734). DOI: 10.1002/ana.25734

Received Sep 16, 2019, and in revised form Mar 24, 2020. Accepted for publication Mar 26, 2020.

Address correspondence to Dr Friederike Irmen, Department of Neurology, Charité – Universitätsmedizin Berlin, corporate member of Freie Universität Berlin, Humboldt-Universität zu Berlin, and Berlin Institute of Health, Berlin, Germany. E-mail: [friederike.irmen@charite.de](mailto:friederike.irmen@charite.de)

<sup>†</sup>These authors contributed equally to this paper.

From the <sup>1</sup>Department of Neurology, Charité – Universitätsmedizin Berlin, corporate member of Freie Universität Berlin, Humboldt-Universität zu Berlin, and Berlin Institute of Health, Berlin, Germany; <sup>2</sup>Berlin School of Mind and Brain, Humboldt-Universität zu Berlin, Berlin, Germany; <sup>3</sup>Department of Biological Psychology and Cognitive Neuroscience, Freie Universität Berlin, Berlin, Germany; <sup>4</sup>Systems Neuroscience Group, QIMR Berghofer Medical Research Institute, Herston, Australia; <sup>5</sup>Queensland Brain Institute, University of Queensland, St. Lucia, Australia; <sup>6</sup>Max Planck UCL Centre for Computational Psychiatry and Ageing Research, Max Planck Institute for Human Development, Berlin, Germany; <sup>7</sup>Center for Lifespan Psychology, Max Planck Institute for Human Development, Berlin, Germany; <sup>8</sup>Faculty of Medicine and University Hospital Cologne, Department of Neurology, University of Cologne, Cologne, Germany; <sup>9</sup>Department of Stereotactic and Functional Neurosurgery, University Hospital Cologne, Cologne, Germany; <sup>10</sup>Department of Neurosurgery, Charité – Universitätsmedizin Berlin, corporate member of Freie Universität Berlin, Humboldt-Universität zu Berlin, and Berlin Institute of Health, Berlin, Germany; and <sup>11</sup>Deutsches Zentrum für Neurodegenerative Erkrankungen, Berlin, Germany

Additional supporting information can be found in the online version of this article.

Deep brain stimulation (DBS) of the subthalamic nucleus (STN) provides relief of motor symptoms in movement disorders, such as Parkinson's disease (PD), by exerting influence on focal target structures and distributed brain networks.<sup>1</sup> A strong relationship between connectivity profiles of DBS electrodes and clinical improvement has been shown in PD<sup>2</sup> and recently in patients with obsessive compulsive disorder.<sup>3</sup> Although Horn et al<sup>2</sup> describe the structural connectivity profile associated with motor improvement in PD, little is known on how structural connectivity impacts non-motor DBS effects. Currently accepted theoretical frameworks postulate that non-motor symptoms following DBS stimulation of basal ganglia targets originate from the modulation of overlapping cortex-basal ganglia motor and non-motor loops.<sup>4</sup> In PD, non-motor DBS-effects have been described in various domains, including autonomic function, sleep, cognition, and mood.<sup>5–9</sup> In the affective domain, in addition to postoperative hypomania,<sup>10</sup> acute depression can be a side effect of STN-DBS in patients with PD<sup>11,12</sup> with a prevalence of about 20 to 25%<sup>13</sup> despite slight improvement after 6 months. Hence, STN-DBS has been reported to improve, worsen, or to have no effect<sup>9</sup> on symptoms of depression or anxiety. However, unlike mania, postoperative depressive symptoms have rarely been associated with sensorimotor STN stimulation itself but rather with too fast tapering of dopaminergic medication<sup>14</sup> and stimulation of more ventral STN territory or even zona incerta stimulation.<sup>13,15,16</sup> Indeed, the precise local placement of DBS electrodes impacts non-motor DBS effects<sup>17,18</sup> and modulation of remote brain regions involved in affective processing might play a crucial role on how affective symptoms develop after surgery.

In this study, we follow up on the research of Horn et al<sup>2</sup> by investigating the impact of electrode placement and associated structural connectivity on changes in depressive symptoms following STN-DBS. To this end, we reconstructed electrode placement in 80 patients with PD from 2 international DBS centers and estimated their structural connectivity profiles using an age-matched normative connectome that was acquired in a different sample of patients with PD. Based on these connectivity profiles, we calculated models that could explain and cross-predict worsening or improvement in depressive symptoms, as measured with the Beck Depression Inventory-Second Edition (BDI-II).<sup>19</sup> Finally, we validated these models using a testing dataset of 36 patients with PD from a third DBS center.

## Materials and Methods

### Patient Cohorts and Imaging

A total of 121 patients from 3 DBS centers (Berlin [BER]: n = 32; Queensland [QU]: n = 49; and Cologne [CGN]: n = 40) were included in this retrospective study (age

62 ± 9 years, 43 women; detailed clinical data in Supplementary Appendix S1). Data from BER and QU were used to form the training and cross-validation datasets to identify structural connectivity associated with mood changes after DBS surgery. Data from CGN was used as a test dataset to validate the established model. Five patients were excluded from the analyses for the following reasons: 1 patient (QU) due to incomplete data, 2 patients (CGN) due to unilateral ventralis intermedius (VIM; instead of STN) stimulation, and 2 patients (CGN) due to clinically relevant psychiatric comorbidities that were pharmacologically treated in the same timeframe in which BDI-II changes were assessed. Table summarizes the sample characteristics of the final cohort (n = 116).

All patients underwent stereotactic DBS surgery for treatment of PD (surgical methods described elsewhere<sup>20</sup>) and received bilateral DBS electrodes (n = 42 model 3389; Medtronic, Minneapolis, MN; n = 31 Boston Scientific Vercise; n = 36 Boston Scientific Vercise Cartesia Directional; and n = 7 St. Jude Infinity Directional model 6172). Structural abnormalities were excluded using preoperative magnetic resonance imaging (MRI). Clinically significant psychiatric symptomatology and cognitive deficits (defined as deficient performance in Mini-Mental State Examination score or multidomain deficits in neuropsychological tests, such as features of PD dementia) were assessed by psychiatric evaluation and neuropsychological testing as exclusion criteria prior to surgery. In all patients, lead placement was validated using microelectrode recordings during surgery, intraoperative macrostimulation, and postoperative imaging. In all 3 DBS centers, quality of pre-operative and postoperative MRI and computed tomography (CT) data was controlled by meticulous visual inspection during stereotactic planning by an interdisciplinary team of neuroradiologists, neurologists, and neurosurgeons. In case of even slight movement artifacts that reduced image quality in a patient, image acquisition was repeated under general anesthesia before surgery. Depressive symptoms were recorded prior to surgery and postoperatively (after 7.56 ± 2.9 months [ie, M ± SD throughout the paper], when DBS settings had been titrated intensively and stable settings have been reached) using BDI-II (cutoff values 0–13: minimal depression; 14–19: mild depression; 20–28: moderate depression; and >29: severe depression). The BDI-II has been validated as a reliable tool for assessment of depressive symptoms in PD despite its disadvantage of potentially biased responses due to face validity. However, it has the practical advantage of an easy and fast administration and is, therefore, routinely acquired in DBS care units, and widely used in studies assessing DBS effects.<sup>21</sup> To control for covariates, sex, levodopa equivalent daily dosage (LEDD), LEDD of dopamine agonists (LEDD-DA), and Unified Parkinson's Disease Rating Scale Part III (UPDRS-III) ON medication were recorded pre-operatively and postoperatively ON DBS in all patients. UPDRS-III data OFF medication was only available for the BER cohort. The study was approved by the local ethics committee at each site and carried out in accordance with the Declaration of Helsinki.

### Localization of DBS Electrodes

DBS electrodes were localized using the advanced processing pipeline<sup>20</sup> in Lead-DBS (www.lead-dbs.org<sup>20</sup>). In short, postoperative

TABLE. Sample Characteristics

	Berlin		Queensland		Cologne		Total	
N	32		48		36		116	
Sex	10F	22M	15F	33M	18F	18M	43F	73M
	M	SD	M	SD	M	SD	M	SD
Age, yr	61	9	62	9	62	8	62	9
Disease duration, yr	10	5	8	4	10	3	9	4
Months postsurgery	12		6		6		7	
BDI-II (Baseline)	11.56	6.15	11.06	4.69	7.00	4.22	9.94	5.41
BDI-II (Postop)	11.56	7.33	8.45*	5.60	7.00	5.76	8.96	6.43
UPDRS-III (Baseline, MED ON)	20.78	10.16	37.46	15.26	17.78	9.75	26.75	15.45
UPDRS-III (ON DBS, MED ON)	19.26	13.55	33.95	12.94	17.00	8.79	24.85	14.44
LEDD-reduction (%)	46.06*	40.06	68.98*	22.75	48.27*	18.66	56.32*	29.70

\*Significant change compared to baseline.  
BDI-II = delta change in Beck's depression inventory (baseline = pre-operative; postop = post-DBS surgery); LEDD = levodopa-equivalent daily dosage; M = mean; UPDRS-III = Unified Parkinson's disease rating scale III (baseline = pre-operative; Postop = post-DBS surgery ON medication).

CT or MRI were linearly coregistered to pre-operative MRI using advanced normalization tools (ANTs; [stnava.github.io/ANTs/](https://stnava.github.io/ANTs/)). Co-registrations were inspected and refined if needed. A brain shift correction step was applied as implemented in Lead-DBS. All pre-operative volumes were used to estimate a precise multispectral normalization to ICBM 2009b NLIN asymmetric ("MNI") space applying the ANTs SyN Diffeomorphic Mapping using the preset "effective: low variance default + subcortical refinement." In some patients where this strategy failed, a multispectral implementation of the Unified Segmentation approach (SPM12; <http://www.fil.ion.ucl.ac.uk/spm/>) was applied. These 2 methods are available as presets in Lead-DBS and were top performers to segment the STN with precision comparable to manual expert segmentations in a recent comparative study.<sup>22</sup> DBS contacts were automatically pre-reconstructed using PaCER<sup>23</sup> or the TRAC/CORE approach and manually refined if needed.<sup>20</sup> For segmented leads, the orientation of electrode segments was reconstructed using the Directional Orientation Detection (DiODE) algorithm.<sup>24</sup>

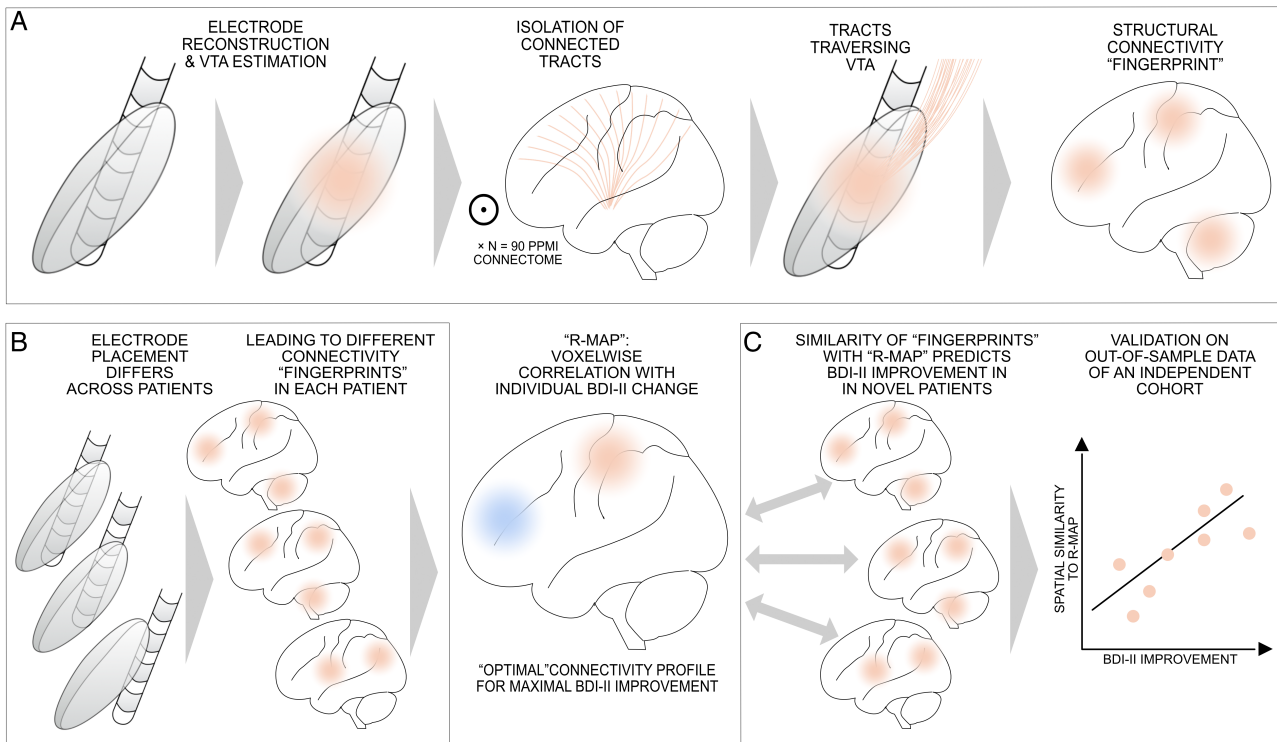
### Volume of Tissue Activated and Connectivity Estimation

Figure 1 provides an overview of the methodology. The volume of tissue activated (VTA) was calculated using default settings in Lead-DBS applying a Finite Element Method (FEM)-based model.<sup>2</sup> This model estimates the E-field (ie, the gradient distribution of the electrical charge in space measured in V/mm) on a tetrahedral mesh that differentiates 4 compartments (grey and

white matter, electrode contacts, and insulation). Grey matter was defined by key structures (STN, internal and external pallidum, and red nucleus) of the DISTAL atlas.<sup>25</sup> The resulting gradient vector magnitude was thresholded at a heuristic value of 0.2V/mm to generate the VTA.<sup>2</sup>

Recently, it has been shown that the use of binary VTAs (modeling all-or-nothing activations) explained slightly less variance in clinical outcomes in direct comparison to the use of weighted VTAs, such as E-field gradient vector magnitudes.<sup>20</sup> Binary VTAs are based on specific thresholds that assume a certain type of axon diameter and orientation and do not grasp the anatomic complexity of the subcortex.<sup>26</sup> To account for this general limitation of the VTA concept, we repeated all analyses using the unthresholded E-field magnitude instead of the VTAs.<sup>27</sup>

Whole-brain structural connectivity profiles seeding from bilateral VTAs or E-fields were estimated using a PD group connectome that is based on publicly available data (Parkinson's Progression Markers Initiative [PPMI]; [www.ppmi-info.org](http://www.ppmi-info.org)). This PPMI normative connectome of patients with PD (n = 90; age 61.38 ± 10.42; 28 women) was priorly computed<sup>25</sup> and has been used in context of DBS multiple times.<sup>2,27,28</sup> For each patient, fibers passing through the VTA or a non-zero voxel of the E-field were selected from this normative connectome and projected onto a voxelized volume in standard space (1mm isotropic resolution) while keeping count of the fibers traversing each voxel. In the VTA-based analyses, the number of fibers



**FIGURE 1:** Overview of applied methods. (A) In each patient, electrodes were localized and volumes of tissue activated (VTAs) were calculated in standard stereotactic space using Lead-DBS software. From a normative Parkinson's disease connectome (N = 90 Parkinson's Progression Markers Initiative [PPMI] datasets), tracts that traversed through each patient's VTA were selected and projected to the brain as fiber density maps. These maps represent the structural connectivity "fingerprint" seeding from each VTA. (B) Varying electrode placement leads to different connectivity fingerprints in each patient. Across the group of patients, these fingerprints are used to generate a model of connectivity that is associated with maximal Beck Depression Inventory-Second Edition (BDI-II) improvement by voxel-wise correlation ("R-Map"). (C) The R-Map represents a model that denotes how electrodes should be connected to result in maximal BDI-II improvement. When comparing each novel patient's fingerprint with this model (by means of spatial correlation), individual BDI-II improvement can be predicted. Crucially, this is done to predict improvement in out-of-sample data (ie, across cohorts or in a leave-one-out fashion throughout the manuscript). This means that the R-map is never informed by the predicted patient's structural connectivity fingerprint.

traversing each voxel was denoted (resulting in fiber-density maps). In the E-field-based analyses, each fiber received the weight of the maximal E-field magnitude of its passage and fiber densities were weighted by these values.

### Modeling Connectivity-Driven Mood Changes

Structural connectivity strength (ie, the number of fibers between VTA and each voxel) was Spearman rank-correlated with BDI-II change [pre-operative and postoperative], which resulted in a connectivity map that showed positive or negative associations with BDI-II improvement. In the following, these types of maps are referred to as R-maps (because they denote Spearman's correlation coefficients in each voxel). Spearman's correlation was used because tractography results are highly non-Gaussian distributed and rather follow an exponential distribution.<sup>29</sup> All analyses were carried out in Matlab (The Mathworks, Natwick, MA). We used randomized permutation tests (5,000 permutations) to test for significance (at a 5% level) and used Spearman's correlation coefficients throughout all analyses.

**Validation of the Training Dataset.** One R-map for each subset (BER and QU) was calculated. R-maps were then used to predict BDI-II changes in the other subset (ie, cross-predicting between QU ↔ BER cohorts) by spatial correlation between the R-map (model) and the connectivity profile seeding from the VTAs in each patient. This was done across voxels with an absolute Spearman's R-value of >0.1 on each R-map. For example, the R-map (model) was calculated across the BER sample and voxels with an absolute  $R \geq 0.1$  were spatially correlated with connectivity maps in the QU sample. For each patient in the QU cohort, this led to one R-value coding for spatial similarity to the model. These R-values were then correlated with empirical BDI-II changes. These head-to-head comparisons show direct relationships between BDI-II changes and the structural connectivity profiles of DBS electrodes. To further investigate their relationship with further clinical variables, the structural connectivity predictor was fed into regression models that included additional clinical information. This was done to analyze whether



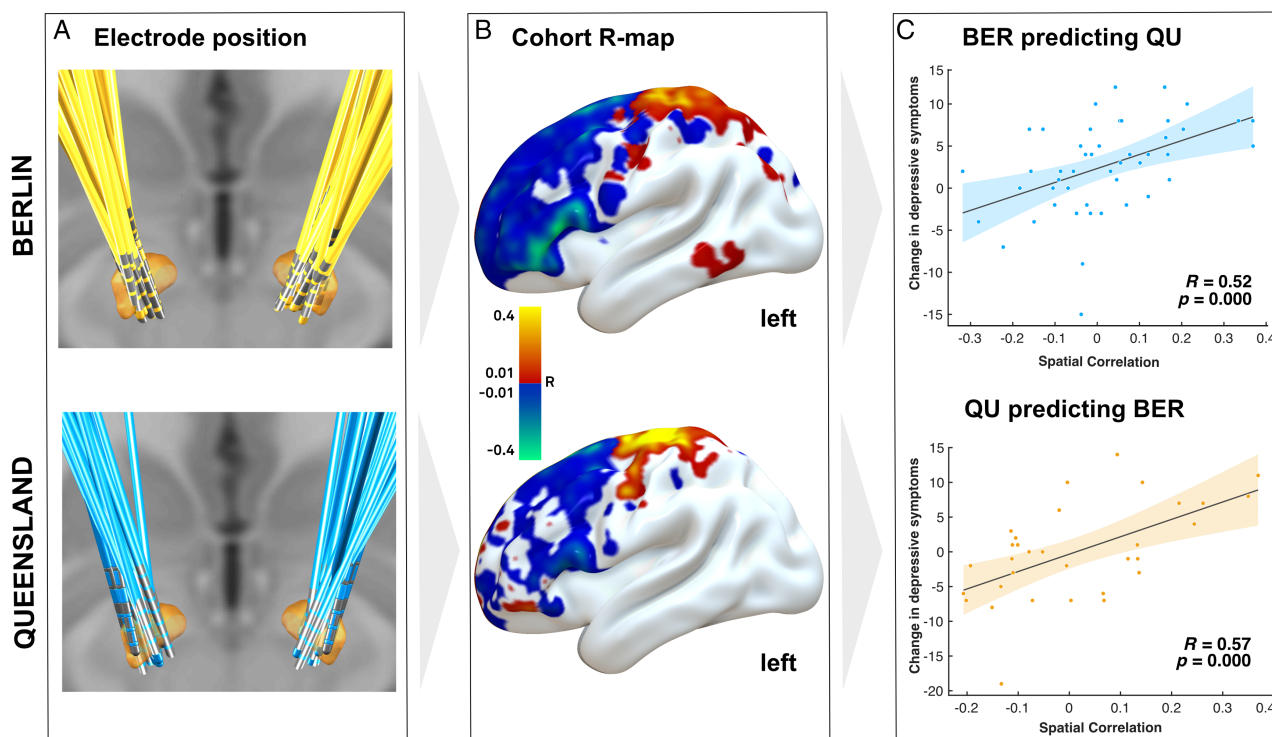


**FIGURE 2:** Structural connectivity predicting change in depressive symptoms in the training dataset ( $N = 80$ ). (A) Electrode position for the two cohorts from Berlin and Queensland. (B) Each cohort's R-Map represents the association with change in depressive symptoms under subthalamic nucleus deep brain stimulation (STN-DBS). Negative (blue) areas of the left hemisphere relate to worsening of depressive symptoms. R-Maps revealed a significant association between worsening of depressive symptoms after STN-DBS and connectivity to left dorsolateral prefrontal cortex (PFC). (C1) Based on the R-Map from the Berlin cohort, depressive symptoms in the Queensland cohort could be significantly predicted and vice versa (C2). R-Maps are presented smoothed with a 3mm full-width half-maximum Gaussian kernel.

structural connectivity significantly explained variance above and beyond other clinical variables.

An additional leave-one-out cross-validation (ie, data from Patients 1–79 was used to predict Patient 80 and so on) across the training sample (BER/QU combined) was carried out to test whether similarity to the specific structural connectivity profile of the training set (which is denoted by the R-map) could significantly predict absolute BDI-II change. Furthermore, we validated the results by carrying out the analyses again (1) based on the E-field instead of VTA and (2) using the percentage BDI-II change relative to baseline instead of the absolute BDI change. Moreover, to test for potential lateralization of connectivity profile, we calculated analyses for left and right VTAs separately.

**Prediction of the Test Dataset.** In the same fashion as the cross-prediction between the subcohorts of the training dataset, a joint R-map for the entire training/cross-validation set (BER + QU) was generated, which was used to predict BDI-II change in patients of the test dataset (CGN).

**Testing Robustness of the Model across the Entire Sample.** We applied the leave-one-out cross-validation across the whole dataset (ie, data from Patients 1–115 was

used to predict Patient 116 and so on). Finally, to control for the effect of sex, postoperative LEDD, LEDD-DA, and UPDRS-III reduction, those variables were included in the prediction models as covariates.

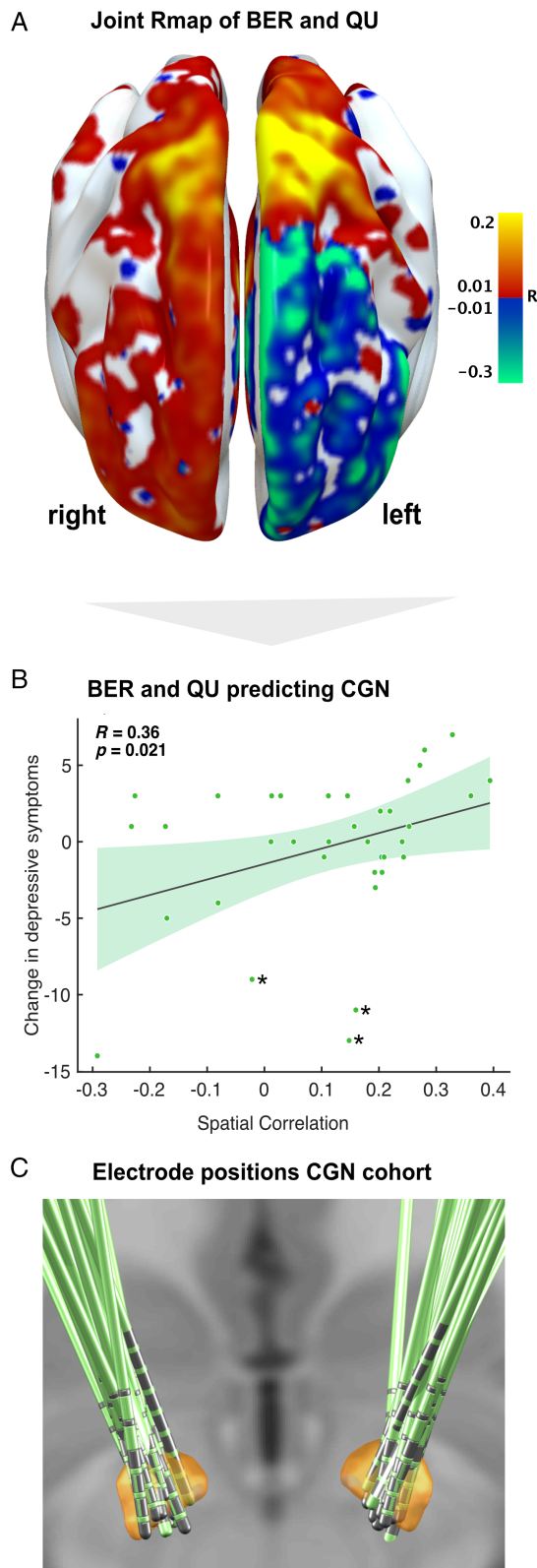
### Isolation of Fibertracts that are Discriminative for Mood Changes

In an additional analysis, we sought to identify tracts that could discriminate patients with positive from those with negative BDI-II change. For each fibertract in the normative connectome, its accumulative E-field vector magnitude while passing by each patient's electrode was calculated. This value was then Spearman rank-correlated with each patient's clinical change in depressive symptoms. Thus, a fibertract that passed close to active contacts of patients who had BDI-II improvement but far from active contacts in patients who had BDI-II worsening would receive a high Spearman's R-value (and tracts exhibiting the inverse property received a highly negative R-value). These R-values were used to color-code fibertracts that were positively and negatively predictive of BDI-II improvement. This analysis was expected to show identical (or highly similar results) as the "R-map" method explained above but with the advantage of working on a tract-by-tract basis (instead of a voxel-wise fashion). Thus, it is ideal to visualize the actual fibertracts that were predictive of change in depressive symptoms.

## Results

### Clinical Data

Disease duration in the entire sample ( $n = 116$ ; see Table; Supplementary Appendix S1) was  $9.55 \pm 4.45$  years. DBS



lead placement was similar across all 3 cohorts (Figs 2A, 3C). Motor improvement with DBS was significant although measured ON medication reaching an average DBS response of  $27.56 \pm 8.37\%$  as measured by the UPDRS-III. Pre-operative LEDD was  $1,142.46 \pm 567.47\text{mg}$  as compared to postoperative  $464.45 \pm 291.37\text{mg}$  ( $56.31 \pm 29.71\%$  reduction) with a contribution of dopamine agonists of  $191.06 \pm 16.62\text{mg}$  pre-operatively and  $107.51 \pm 10.73\text{mg}$  postoperatively. Total LEDD, LEDD-DA, and UPDRS-III reduction were not significantly different in training and test datasets ( $p > 0.05$  for all 3 variables; see Table). According to BDI-II scores before DBS surgery, 35 patients showed signs of mild depression, and 6 of moderate depression, but none were classified severely depressed (all BDI-II scores  $< 29$ ). Postoperative BDI-II assessments classified 31 patients as mildly depressed (of these twelve patients were classified not depressed prior to surgery), seven patients as moderately depressed (of these two patients had been mildly depressed before and two patients had been classified not depressed before surgery) and 2 patients as severely depressed (one had been classified as not depressed prior to surgery, the other had been moderately depressed). On average, BDI-II scores decreased from  $9.94 \pm 5.41$  to  $8.96 \pm 6.43$  (on average by  $0.97 \pm 5.86$  points) postoperatively, ie, there was an overall reduction in BDI-II of  $3.34 \pm 87.48\%$  but the difference was not significant. Importantly, scores improved in 65 patients and worsened in 41 patients. Ten patients showed no change in BDI. Stimulation amplitudes between left and right hemispherical DBS electrodes (left:  $2.46 \pm 0.79$  mA; right:  $2.58 \pm 0.83$  mA) were not significantly different ( $p = 0.22$ ).

### Connectivity Related to DBS-Induced Mood Changes

We identified a VTA-based structural connectivity map (R-map) predictive of postoperative BDI-II change in the training dataset (Fig 2B). The more fibers connected a patient's VTA to the positive areas (warm colors) of this map, the more their depressive symptoms improved postoperatively. On the contrary, the more a patient's VTA was

**FIGURE 3: R-map of the training-dataset and prediction of test dataset. (A) R-Map of the training dataset. Negative (blue) areas represent association with worsening of depressive symptoms, whereas positive (red) areas represent association with improvement of depressive symptoms under subthalamic nucleus deep brain stimulation (STN-DBS). The R-Map is presented smoothed with a 3mm full-width half-maximum Gaussian kernel to increase signal-to-noise ratio. (B) The R-Map of the training dataset (Berlin-Queensland model) significantly predicted change in depressive symptoms in the test-dataset (Cologne). (C) Electrode positions of the test dataset within the subthalamic nucleus (STN).**

structurally connected to the negative areas (cold colors) of this map, the more their depressive symptoms worsened.

**Validation of the Training Dataset.** The R-maps of the 2 subcohorts in the training dataset were similar: on the right hemisphere of the R-map, connectivity to motor and prefrontal regions was associated with depressive symptom improvement. On the left hemisphere, however, connectivity to prefrontal cortex (PFC), including the dorsolateral PFC (dlPFC) was strongly associated with worsening of depressive symptoms, whereas connectivity to sensorimotor and superior parietal areas was associated with symptom improvement (Fig 2B). Cross-predictions were significant (ie, the R-map based on BER-data could predict BDI-II changes in the QU dataset; Fig 2C,  $R = 0.52$ ,  $p < 0.0001$ ) and vice versa ( $R = 0.57$ ,  $p < 0.0001$ ). In a leave-one-out cross-validation across the training sample (BER/QU combined), similarity to this specific structural connectivity profile (R-map) could significantly predict absolute BDI-II change ( $R = 0.26$ ,  $p = 0.01$ ) even when basing structural connectivity profiles on the E-field instead of VTA ( $R = 0.24$ ,  $p = 0.015$ ) or when using the percentage BDI-II change relative to baseline instead of absolute BDI change ( $R = 0.20$ ,  $p = 0.04$ ). To test whether the effect was lateralized to either hemisphere, we repeated analyses for left and right VTAs separately and found that connectivity on either hemisphere alone was predictive for BDI-II change (right:  $R = 0.347$ ,  $p = 0.002$ ; left:  $R = 0.359$ ,  $p = 0.001$ , Fig 5D). To rule out a systematic left–right bias of VTA placement, displacement of image centering or asymmetries in the normative connectome, we recalculated the R-map after flipping the VTAs between left and right hemisphere while not flipping the connectome. The results remained stable, producing the same (lateralized, but mirrored) findings. This control analysis could largely rule out systematic left–right biases in our analysis pipeline.

**Prediction of the Test Dataset.** The R-map based on the whole training set (BER/QU combined) was used to predict BDI-II change in the independent test dataset (CGN) by calculating spatial similarity between each CGN-patient's connectivity profile with the BER/QU R-map (Fig 3A). This validated our results as a significant correlation was observed (Fig 3B,  $R = 0.36$ ,  $p = 0.012$ ). The test dataset (CGN) had been isolated from all model-selection processes and was used as a final confirmation after cross-validation between BER and QU. Still, the validation also yielded similarly positive predictions when subsequently using any other cohort as test dataset (QU/CGN  $\rightarrow$  BER:  $R = 0.38$ ,  $p = 0.009$ ; BER/CGN  $\rightarrow$  QU:  $R = 0.20$ ,  $p = 0.06$ ). In the CGN test dataset, some specific features were noted: Patients

#10 and #19 were diagnosed with comorbid depression and anxiety disorder at baseline; and Patient #13 reported pain and relatedly negative mood. Those 3 patients are marked with an asterisk in Fig 3B. Importantly, excluding those patients still rendered the prediction significant ( $R = 0.28$ ,  $p = 0.047$ ).

**Testing Robustness of the Model across the Entire Sample.** As final step, we created one final R-map across all available data (BER/QU/CGN,  $n = 116$ ), which was predictive for BDI-II change in all three cohorts (Fig 4A). This final R-map yielded significant predictions in a leave-one-out cross validation analysis (Fig 4B,  $R = 0.33$ ,  $p \leq 0.001$ ). It remained significant when including sex, postoperative LEDD and LEDD-DA reduction, and percentage UPDRS-III change (postoperative–preoperative ON medication) as covariates and correcting for cohort in a joint general linear model ( $R^2 = 0.21$ ,  $F_{(112,104)} = 3.88$ ,  $p = 0.001$ ). Thus, this final model explained 21% of variance in BDI-II change based on clinical covariates and structural connectivity profiles across the whole group of subjects. The model remained significant when leaving any one cohort out (leaving out BER:  $R^2 = 0.18$ ,  $F_{(82,76)} = 3.25$ ,  $p = 0.01$ ; leaving out QU:  $R^2 = 0.29$ ,  $F_{(64,58)} = 4.75$ ,  $p = 0.001$ ; and leaving out CGN:  $R^2 = 0.20$ ,  $F_{(78,72)} = 3.71$ ,  $p = 0.005$ ). To test for the effect of UPDRS-III change induced by DBS (% difference OFF medication), a subanalysis was performed for the entire BER sample ( $n = 32$ ), where this data was available, and structural connectivity remained a significant predictor of BDI-II change ( $R^2 = 0.19$ ,  $p = 0.05$ ).

**Focal Impact on STN Segments.** To supplement the connectivity analyses, the number of voxels inside versus outside the STN and within motor versus nonmotor STN, that were stimulated by the VTAs were counted for each patient and correlated with BDI change. The more VTA-voxels lay inside the STN, the higher BDI-II scores improved ( $R = 0.285$ ,  $p = 0.002$ ), no matter if VTA stimulated motor or nonmotor STN segments ( $R = 0.267$ ,  $p = 0.002$  and  $R = 0.197$ ,  $p = 0.034$ ). The number of VTA-voxels outside the STN was not predictive for BDI-II change ( $R = -0.129$ ,  $p = 0.166$ ), suggesting that stimulation of specific fibers passing by the STN would explain BDI-II worsening, rather than unspecific stimulation of non-STN tissue.

**Individual Differences.** We demonstrate that the connectivity profile shown in Fig 4 was associated with changes on the BDI-II score across DBS centers, surgeons, and cohorts. However, on a single patient level, changes showed a root-mean-square (RMS) error of  $4.11 \pm 3.51$  points in the leave-one-out cross-validation.

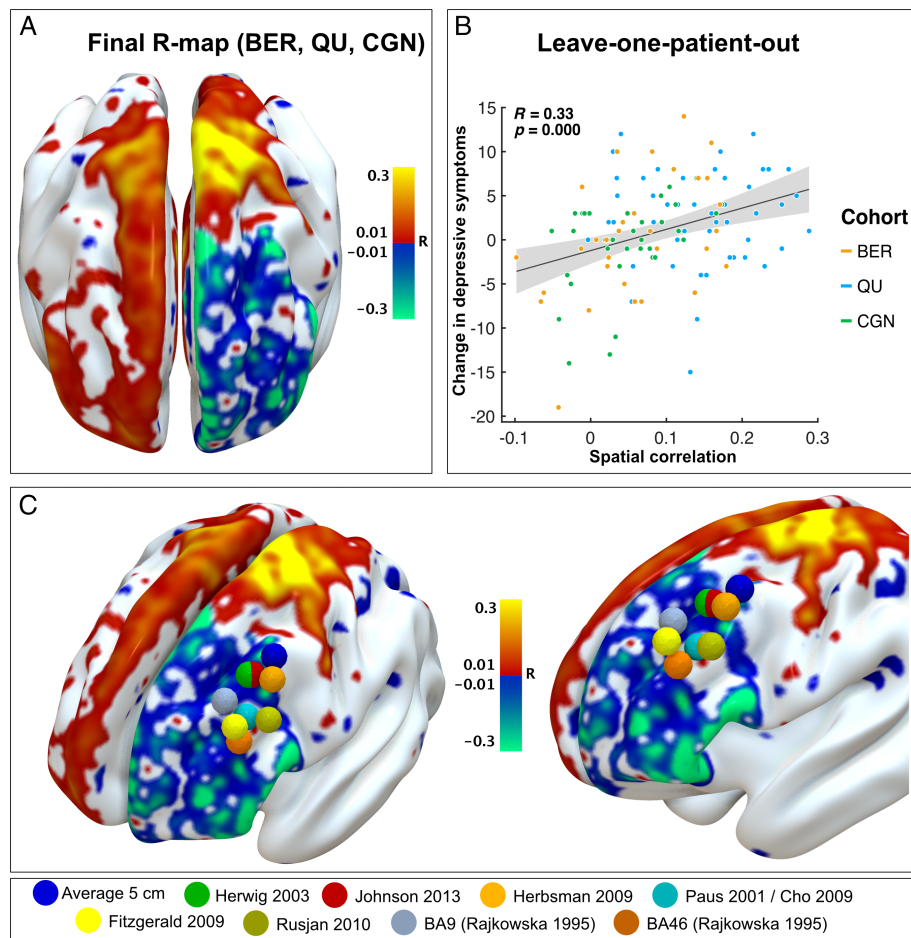


**FIGURE 4:** Final R-Map validation across all patients and proximity to transcranial magnet stimulation (TMS) targets. (A) R-Map associated with change of depressive symptoms across all patients ( $n = 116$ ). (B) Validation of the model using a leaving-one-out design. (C) Literature-based repetitive TMS (rTMS) targets for treatment of depression superimposed on final R-Map. R-Maps are presented smoothed with a 3mm full-width half-maximum Gaussian kernel to increase signal-to-noise ratio.

**Confounding Variables.** In order to visualize possible confounding variables, we calculated the R-maps for subsamples of our patient cohorts: Fig 5 shows that the structural connectivity patterns predictive for postoperative BDI-II worsening remains in the left prefrontal cortex for (A) patients who were not depressed before surgery ( $\text{BDI-II} \leq 13$ ,  $n = 86$ ); (B) patients who were mildly or moderately depressed before surgery ( $\text{BDI-II} > 13$ ,  $n = 30$ ); and (C) patients who were not treated with dopamine agonists before or after DBS surgery ( $n = 26$ ).

### Fibertracts Related to Mood Changes

An additional analysis was carried out to identify the actual tracts (instead of their cortical projection sites) the modulation of which was correlated with BDI-II improvement. This was done on a tract-by-tract instead of voxel-wise basis and further confirmed our results using a different analysis pathway. Crucially, this data-driven analysis revealed largely more tracts on the left hemisphere than on the right hemisphere, again suggesting an impact of left DBS stimulation on

change of depressive symptoms (Fig 6A). Using lower thresholds, the pattern was similar between the 2 hemispheres but left hemispheric tracts were more predictive of BDI-II change and predictive tracts were found in larger quantities. The analysis revealed that the positively and negatively associated tracts seemed to differ in their anatomic course in that the negatively associated tract passed by the STN medially and at level of its limbic/associative functional zone, whereas the positively correlated tract passed through and slightly lateral to the motor STN (Fig 6B,C). Moreover, as can be seen in Fig 6D, at level of the brainstem, the negatively associated tract traversed closely to the left dorsal raphe nucleus.

### Discussion

In this study, we estimated structural connectivity that could predict changes in depressive symptoms following STN-DBS in PD. We identified a distinct connectivity pattern linking worsening of depressive symptoms under STN-DBS to left prefrontal connectivity. This connectivity profile predicted



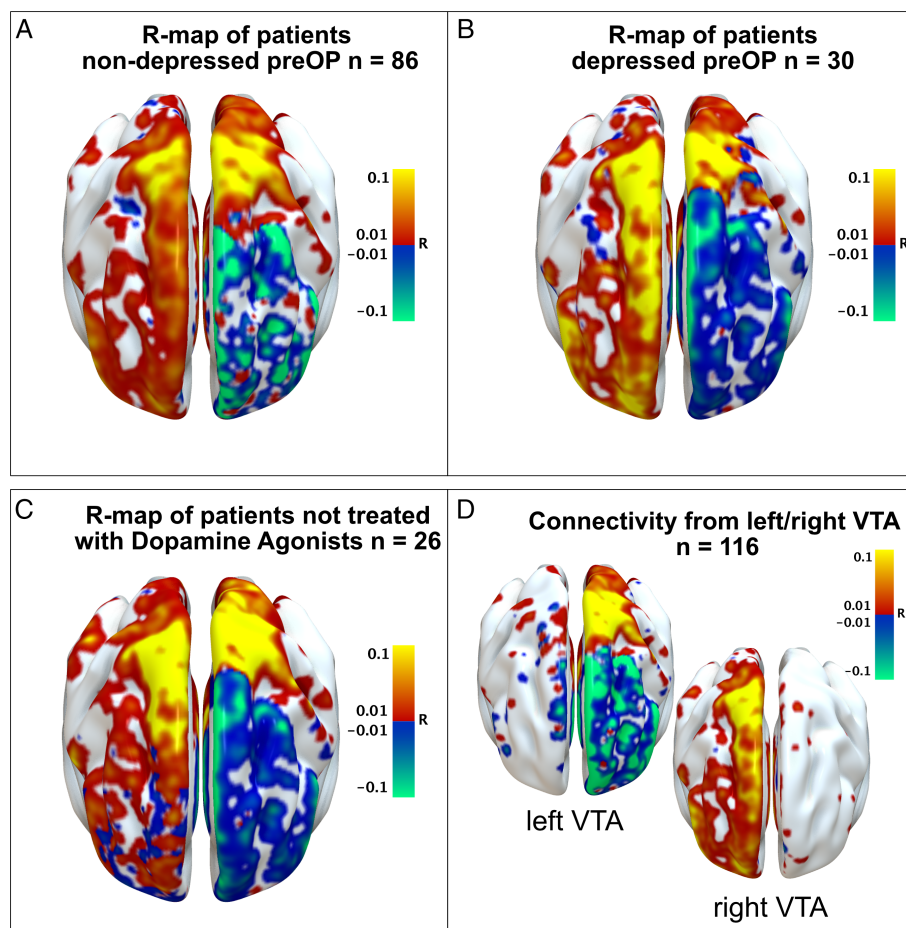


**FIGURE 5:** R-maps of subsamples of patients with Parkinson's disease (PD). The structural connectivity pattern that is predictive for Beck Depression Inventory-Second Edition (BDI-II) change remains stable in subanalyses on (A) patients that were not depressed before surgery ( $\text{BDI-II} \leq 13$ ,  $n = 86$ ); (B) patients that were mildly or moderately depressed before surgery ( $\text{BDI-II} > 13$ ,  $n = 30$ ); and (C) patients that were not treated with dopamine agonists before or after deep brain stimulation (DBS) surgery ( $n = 26$ ). (D) When carrying out the analyses for left and right volumes of tissue activated (VTAs) separately, the connectivity pattern also exhibited the same spatial profile.

clinical variance across cohorts. Specifically, left-hemispheric modulation of fibers that traverse the anteromedial STN connecting to the PFC predicted worsening of depressive symptoms.

A common assumption about DBS-induced affective changes is their relation to rapid withdrawal of dopaminergic replacement therapy after surgery, which increases anhedonia induced by affective network dysregulation.<sup>14</sup> Although this factor explains acute and subacute postoperative affective changes, in our large multicenter sample, LEDD and LEDD-DA reduction did not explain BDI-II change after 6–12 months. Perhaps this relates to clinicians addressing this potential risk factor for depression during long-term follow-up. Others have also reported a lack of correlation between LEDD reduction and non-motor PD symptoms such as apathy and mood.<sup>6,8</sup> However, the general notion is that STN-DBS mimics the action of dopaminergic agents<sup>10</sup> and acute stimulation more likely leads to hypomania than depression.<sup>10,30,31</sup> Interestingly, long-term improvement in motor

symptoms supposedly inducing secondary improvements of mood<sup>2</sup> did not change the predictive value of connectivity for depressive symptom change, suggesting that stimulation may influence affective processing more directly (ie, via impact on left PFC).

The association of depressive symptoms and connectivity to left PFC is unsurprising given the vast amount of evidence that has linked depression to frontal lesions: hypoactivity and dysfunction of left PFC is commonly observed in patients with depression.<sup>32</sup> Moreover, depressive symptoms increase gradually after left dlPFC traumatic brain injury and stroke depending on the extent of damage and network impact.<sup>33</sup> Indeed, large-scale network effects, hemispheric asymmetries, and connectivity play an important role in the development of depressive symptoms<sup>34</sup> (eg, post-stroke depression has been linked to altered dlPFC functional connectivity).<sup>35</sup> Functionally, the left dlPFC might regulate negative affect via the frontoparietal cognitive control network.<sup>36</sup> In major

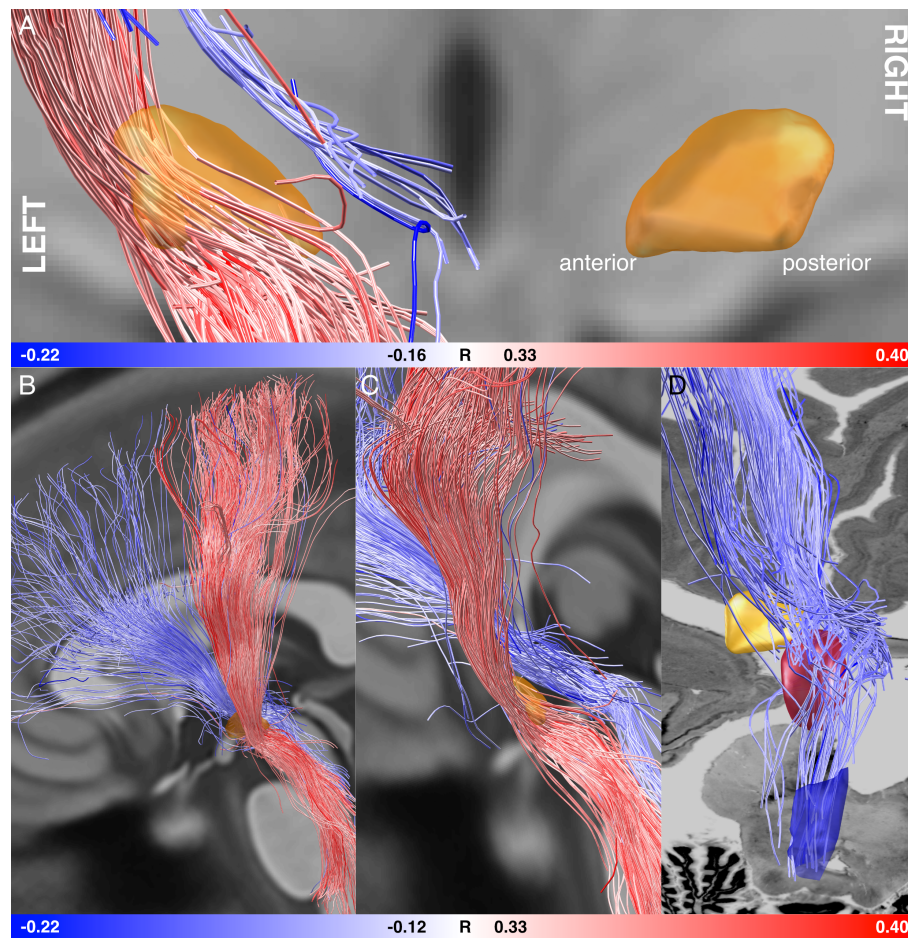


**FIGURE 6:** Fibertracts discriminative of Beck Depression Inventory-Second Edition (BDI-II) improvement when modulated. Red tracts are positively, blue tracts negatively correlated with clinical improvement. STN shown in orange. (A) Coronal view from posterior with both hemispheres. At this threshold level, no fibers on the right hemisphere were associated with clinical improvement but a strong set of both positive and negative fibers were found on the left hemisphere. (B) View from the left and (C) view parallel to the longitudinal axis of the left subthalamic nucleus (STN). Positively and negatively correlated fibertracts seem to be distinct tracts, the positive one passing through the STN and lateral to it, the negative one medial and anteriorly. (D) Superimposed on a section of the BigBrain ultrahigh resolution human brain model,<sup>58</sup> at the level of the brainstem, the negative tract seems to traverse around the red nucleus and may connect to (or originate from) brainstem nuclei, such as the left dorsal raphe nucleus (shown in dark blue as defined by the Harvard Ascending Arousal Network Atlas).

depression, excitability of hypoactive dlPFC tissue<sup>32</sup> is augmented by noninvasive high-frequency repetitive transcranial magnet stimulation (rTMS) leading to symptom amelioration.<sup>37</sup> Although the precise mechanism of dlPFC rTMS in improving depressive symptoms is not fully understood, a role of local and remote network changes and altered PFC connectivity is evident.<sup>38</sup> Interestingly, common targets of rTMS in depression<sup>38</sup> precisely lie within the clusters we find associated with BDI-II worsening under STN-DBS (see Fig 4C).

Concurrently, in this study, worsening of depressive symptoms under STN-DBS was associated with stimulation of fibers connecting prefrontal areas via the subthalamic region to the dorsal mesencephalon and brainstem (Fig 6D). We presume that STN-DBS may disrupt information flow along these fibers. One candidate

brainstem region whose link to the PFC might be accidentally disturbed by DBS leading to depression is the dorsal raphe nucleus (DRN), which, as part of the serotonergic system, is known to impact mood states and which is hypoactive in depression.<sup>39</sup> Indeed, unbalanced prefrontal-DRN connectivity relates to depression<sup>40</sup> and rodent studies have shown that STN-DBS may inhibit serotonergic output from the DRN inducing depression-like behavior.<sup>41</sup> Because direct STN-DRN connections have not been widely described, misplaced STN-DBS may instead disrupt left prefrontal-DRN serotonergic communication by accident,<sup>42</sup> indirectly fostering depressive states. Another candidate neural substrate involved is the ventral tegmental area, which as origin of mesolimbic dopamine projections is pivotal for reward-processing but also plays a role in depression.<sup>43</sup> Finally, our analysis has shown links to larger proportions of



the left prefrontal cortex and did not exclusively delineate its dorsolateral part. Other frontal regions have been proposed to play a role in depressive states in PD.<sup>45</sup>

As mentioned in the introduction, STN-DBS has led to improvements, worsening or no effect on affective symptoms when analyzed on a group level. The same applies to the combined cohort analyzed here. Although depressive symptoms in individuals of the cohort improved and got worse—and for some by large—on a group level, pre-operative and postoperative scores were not significantly different. On a center-by-center level, 1 cohort (QU) significantly improved while the other 2 did not. Our study may provide reason for these conflicting results, which could be based on electrode placements, especially in the left STN. A left electrode position that was more anterior was associated with worsening of affective symptoms. Crucially, this was the case in all 3 cohorts. Thus, depending on surgical practices or slightly differing average targets of each center, differing group effects in reported studies or DBS cohorts could be explained.

A role of the STN itself in affective processing is undisputed.<sup>17</sup> Like the striatum, the STN is a node of convergence of affective, cognitive, and motor input.<sup>4,45</sup> Its activity is modulated through coupling with PFC activity<sup>46</sup> and STN-DBS impacts affective processing.<sup>47</sup> Concurrently, in our data, depressive symptoms improved if predominantly fibers connecting the dorsolateral (motor) STN with the sensorimotor cortex were stimulated (as reported previously<sup>48</sup>). Although STN-sensorimotor-cortex connectivity has primarily been associated with improvements in motor performances, a recent study showed that mood improvement relies on DBS of the motor STN.<sup>49</sup> Similarly, motor STN stimulation can normalize cognitive performance.<sup>50</sup> This implicates the overlapping presence of affective/associative and motor processing neurons in the STN motor segment<sup>4</sup> and suggests that retuning the motor loop may improve non-motor features as well.

Another region to which electrode connectivity predicted improvement of depressive symptoms was the right dlPFC. Current neuroimaging studies speak of reduced left and increased right dlPFC activity associated with depressive symptoms.<sup>51</sup> Although this fits our results, we must emphasize that while evidence for the link between left hypoactive dlPFC and depressive symptoms seems solid, the association between right hyperactive dlPFC and improved mood is weak.<sup>52</sup> The origin and validity of such lateralized effects require further investigation.

Taken together, in the left hemisphere, high-frequency stimulation of fibers in proximity to the anteromedial STN was associated with worsening of

depressive symptoms, whereas stimulation of dorsolateral STN leads to improvement of depressive symptoms in patients with PD. The connectivity profile described in this study may inform surgeons and clinicians in placement and settings of STN-DBS. The present results may help avoid harmful side effects of STN-DBS in patients with PD by considering connectivity to networks guiding these side effects, however, further work fostering a refined understanding of the functionality of PFC-STN connectivity and lateralized impact is key.

As a final consideration, it is important to stress that we believe depression is a system-level disorder: no single brain region or neurotransmitter is the sole driving force but, instead, integrated cortical–subcortical networks play a role.<sup>32</sup> This means the impact of STN-DBS on affective networks based on patients' connectivity profiles is surely not the only factor contributing to changes in depressive symptoms. However, this research may contribute to better understand, avoid, and treat affective side effects like depressive symptoms in patients with STN-DBS.

There are several limitations to our findings. First, differences in the timepoints of assessment of depressive symptoms across DBS centers may have affected our results. There is variance in follow-up timepoints between cohorts, which arose given the retrospective multicenter study design. However, all follow-ups were later than 5 months after surgery when usually a stable effect of DBS parameter settings and medication is reached. Moreover, this variance might have biased our results toward nonsignificance and could also be interpreted as a strength in robustness of results. We do believe, that with our large sample size slight variances in the timepoint of BDI-II assessment did not systematically bias our results.

Second, there is a variation in electrode type in the patients included in this study. This could affect the VTA-model (eg, by respective consideration of constant voltage vs constant current default settings in DBS systems). To circumvent a bias of this factor, we repeated analyses using the unthresholded E-field surrounding electrodes and found similar results.

Third, we used an age and disease-matched group connectome that was based on data acquired in patients with PD enrolled in the PPMI project, which will not account for individual structural connectivity but instead assumes similar connectivity profiles in all patients. Although this assumption might not hold true in all cases, several recent studies have introduced and validated the method within DBS context.<sup>2,3,28</sup> Beyond practical advantages (where patient-specific connectivity data are often not available and cannot be acquired postoperatively), normative connectomes like the one used here comprise a high number of subjects, which, by averaging, lead to high

signal-to-noise levels and state-of-the-art data quality. Yet, residual movement during the scan might be a potential source of confound on the data quality of the images, which remains a limitation. Moreover, disease stage of patients in the PPMI-connectome differed from our patients in that they were predominantly patients with early stage PD. Although prior research showed that the choice of group connectomes does not largely alter results in the kind of analyses performed here,<sup>2</sup> we still emphasize this limitation.

Fourth, we only had UPDRS-III scores ON medication for most patients and, thus, pre-operative to postoperative comparisons might not reflect the full impact of STN-DBS on motor symptoms. However, a subanalysis of the entire BER sample ( $n = 32$ ), in which UPDRS-III comparison OFF medication was possible, yielded similar results; thus, we believe that structural connectivity remained the strongest predictor for depressive symptom change.

Fifth, we used a general self-rating scale to score depressive symptoms, which does not allow to specify the change in subitems, such as anxiety or apathy. Unfortunately, our study was unable to address DBS-related changes in symptom-specific pattern because the corresponding scores were not available in our cohorts. Thus, future research should compare our results with other symptom clusters.

Sixth, a confound of the present study should be seen in the accuracy of electrode reconstructions. Although it is impossible to estimate an empirical average error without histological postmortem validation of results, we applied a modern pipeline that was explicitly designed for the task. Processing steps included phantom-validated electrode reconstructions,<sup>53</sup> brain shift correction,<sup>20</sup> multispectral nonlinear registrations to target nuclei that were empirically validated,<sup>22</sup> and finite-element method-based estimations of stimulation volumes.<sup>2</sup> Two studies have validated the pipeline using electrophysiological recordings<sup>54,55</sup> and others have demonstrated that results are capable of explaining clinical improvements across patients, DBS centers, and cohorts.<sup>2,3,50,56,57</sup> Still, residual errors of electrode reconstructions cannot be excluded.

Finally, although the connectivity profile associated with depressive symptom changes identified in this study could be reproduced in 3 individual cohorts and cross-validation across DBS centers yielded significant predictions, on an individual level, predictions are not truly useful for clinical practice with an average RMS error of  $4.11 \pm 3.51$ . Thus, our model is not able to predict clinical changes along symptoms covered by the BDI-II score with high precision. Whereas this is a limitation for clinical applicability, the main message of our results may still be useful to inform clinical practice, especially in targeting the left electrode for STN-DBS.

In conclusion, the present results have potential therapeutic value for the refinement of brain stimulation targets. In personalized brain stimulation, identifying proximity to fibers connecting the electrode to the left dlPFC might have prognostic utility in predicting affective changes under STN-DBS. Prospectively, connectivity maps as well as isolated fibertracts can be used in surgical planning to optimize positioning of DBS leads. Furthermore, with directional leads, the electric field could be steered away from fibertracts anteromedial to the left STN to avoid depressive symptom worsening. Importantly, this study specifically shows that the STN connectivity profiles might have to be treated differently for the right and left hemisphere. However, more work is needed to validate this presumption using patient-specific connectivity. Altogether, our findings contribute to better understand how negative mood effects may originate following STN-DBS and pave the way toward personalized brain stimulation in which individual connectivity profiles and symptom constellations could determine optimal DBS targets.

## Acknowledgments

This study was supported by the Deutsche Forschungsgemeinschaft (DFG grant SPP2041, “Clinical connectomics: a network approach to deep brainstimulation” to A.A.K. as well as Emmy Noether Grant 410169619 to A.H.).

We thank Alexandra Horn for her valuable contribution in the data analysis.

Data used in the preparation of this article were obtained from the Parkinson’s Progression Markers Initiative (PPMI) database ([www.ppmi-info.org/data](http://www.ppmi-info.org/data)). For up-to-date information on the study, visit [www.ppmi-info.org](http://www.ppmi-info.org). PPMI—a public-private partnership—is funded by the Michael J. Fox Foundation for Parkinson’s Research and funding partners, see [www.ppmi-info.org/fundingpartners](http://www.ppmi-info.org/fundingpartners).

## Author Contributions

F.I., A.H., and A.A.K. contributed in the design of the study. All authors contributed to acquisition and analysis of data. F.I., A.H., and A.A.K. drafted the text and prepared the figures. All authors reviewed and revised the manuscript for intellectual content.

## Potential Conflicts of Interest

A.A.K. has received honoraria as speaker for Boston Scientific, Abbott, and Medtronic, all makers for DBS devices, which is not related to the current work. A.H. has received one-time speaker honorarium by Medtronic not related to the current work. J.N.P.S. has received a travel grant by Boston Scientific not related to the current work.

V.V.V. has received honoraria as speaker and/or contributions to advisory board meetings for Boston Scientific, Abbott, and Medtronic, all makers for DBS devices, which is not related to the current work.

## References

- Lozano AM, Lipsman N. Probing and regulating dysfunctional circuits using deep brain stimulation. *Neuron* 2013;77:406–424.
- Horn A, Reich M, Vorwerk J, et al. Connectivity predicts deep brain stimulation outcome in Parkinson disease. *Ann Neurol* 2017;82:67–78.
- Baldermann JC, Melzer C, Zapf A, et al. Connectivity profile predictive of effective deep brain stimulation in obsessive-compulsive disorder. *Biol Psychiatry* 2019;85:735–743. <https://doi.org/10.1016/J.BIOPSYCH.2018.12.019>.
- Haynes WIA, Haber SN. The organization of prefrontal-subthalamic inputs in primates provides an anatomical substrate for both functional specificity and integration: implications for basal ganglia models and deep brain stimulation. *J Neurosci* 2013;33:4804–4814.
- Chaudhuri KR, Schapira AHV. Non-motor symptoms of Parkinson's disease: dopaminergic pathophysiology and treatment. *Lancet Neurol* 2009;8:464–474.
- Dafsari HS, Petry-Schmelzer JN, Ray-Chaudhuri K, et al. Non-motor outcomes of subthalamic stimulation in Parkinson's disease depend on location of active contacts. *Brain Stimul* 2018;11:904–912.
- Dafsari HS, Reddy P, Herchenbach C, et al. Beneficial effects of bilateral subthalamic stimulation on non-motor symptoms in Parkinson's disease. *Brain Stimul* 2016;9:78–85.
- Dafsari HS, Silverdale M, Strack M, et al. Nonmotor symptoms evolution during 24 months of bilateral subthalamic stimulation in Parkinson's disease. *Mov Disord* 2017;33:421–430.
- Fasano A, Daniele A, Albanese A. Treatment of motor and non-motor features of Parkinson's disease with deep brain stimulation. *Lancet Neurol* 2012;11:429–442.
- Volkman J, Daniels C, Witt K. Neuropsychiatric effects of subthalamic neurostimulation in Parkinson disease. *Nat Rev Neurol* 2010;6:487–498.
- Funkiewiez A, Ardouin C, Cools R, et al. Effects of levodopa and subthalamic nucleus stimulation on cognitive and affective functioning in Parkinson's disease. *Mov Disord* 2006;21:1656–1662.
- Voon V, Krack P, Lang AE, et al. A multicentre study on suicide outcomes following subthalamic stimulation for Parkinson's disease. *Brain* 2008;131:2720–2728.
- Witt K, Daniels C, Volkman J. Factors associated with neuropsychiatric side effects after STN-DBS in Parkinson's disease. *Parkinsonism Relat Disord* 2012;18:S168–S170.
- Thobois S, Ardouin C, Lhommée E, et al. Non-motor dopamine withdrawal syndrome after surgery for Parkinson's disease: predictors and underlying mesolimbic denervation. *Brain* 2010;133:1111–1127.
- Okun MS, Fernandez HH, Wu SS, et al. Cognition and mood in Parkinson's disease in subthalamic nucleus versus globus pallidus interna deep brain stimulation: the COMPARE trial. *Ann Neurol* 2009;65:586–595.
- Bejjani B-P, Damier P, Arnulf I, et al. Transient acute depression induced by high-frequency deep-brain stimulation. *N Engl J Med* 1999;340:1476–1480.
- Mallet L, Schupbach M, N'Diaye K, et al. Stimulation of subterritories of the subthalamic nucleus reveals its role in the integration of the emotional and motor aspects of behavior. *Proc Natl Acad Sci* 2007;104:10661–10666.
- Mosley PE, Smith D, Coyne T, et al. The site of stimulation moderates neuropsychiatric symptoms after subthalamic deep brain stimulation for Parkinson's disease. *NeuroImage Clin* 2018;18:996–1006.
- Beck AT, Steer RA, Brown GK. *Manual for the Beck depression inventory-II*. San Antonio, TX: Psychological Corporation, 1996.
- Horn A, Li N, Dembek TA, et al. Lead-DBS v2: towards a comprehensive pipeline for deep brain stimulation imaging. *Neuroimage* 2019;184:293–316.
- Schuepbach WM, Rau J, Knudsen K, et al. Neurostimulation for Parkinson's disease with early motor complications. *N Engl J Med* 2013;368:610–622.
- Ewert S, Horn A, Finkel F, et al. Optimization and comparative evaluation of nonlinear deformation algorithms for atlas-based segmentation of DBS target nuclei. *Neuroimage* 2019;184:586–598.
- Husch A, Petersen MV, Gemmar P, Goncalves J, Hertel F. PaCER - A fully automated method for electrode trajectory and contact reconstruction in deep brain stimulation. *NeuroImage Clin* 2017;17:80–89. <http://doi.org/10.1016/j.nicl.2017.10.004>
- Dembek TA, Hoevels M, Hellerbach A, et al. Directional DBS leads show large deviations from their intended implantation orientation. *Parkinsonism Relat Disord* 2019;67:117–121. <https://doi.org/10.1016/j.parkreldis.2019.08.017>.
- Ewert S, Plettig P, Li N, et al. Toward defining deep brain stimulation targets in MNI space: a subcortical atlas based on multimodal MRI, histology and structural connectivity. *Neuroimage* 2017;170:271–282. <https://doi.org/10.1016/j.neuroimage.2017.05.015>.
- Forstmann BU, de Hollander G, van Maanen L, et al. Towards a mechanistic understanding of the human subcortex. *Nat Rev Neurosci* 2016;18:57.
- Horn A, Wenzel G, Irmen F, et al. Deep brain stimulation induced normalization of the human functional connectome in Parkinson's disease. *Brain* 2019;0:1–15.
- Neumann W-J, Schroll H, de Almeida Marcelino AL, et al. Functional segregation of basal ganglia pathways in Parkinson's disease. *Brain* 2018;141:2655–2669.
- Horn A, Ostwald D, Reiser M, Blankenburg F. The structural-functional connectome and the default mode network of the human brain. *Neuroimage* 2014;102:142–151.
- Castrioto A, Lhommée E, Moro E, Krack P. Mood and behavioural effects of subthalamic stimulation in Parkinson's disease. *Lancet Neurol* 2014;13:287–305.
- Krack P, Hariz MI, Baunez C, et al. Deep brain stimulation: from neurology to psychiatry? *Trends Neurosci* 2010;33:474–484.
- Mayberg HS, Lozano AM, Voon V, et al. Deep brain stimulation for treatment-resistant depression. *Neuron* 2005;45:651–660.
- Grajny K, Pyata H, Spiegel K, et al. Depression symptoms in chronic left hemisphere stroke are related to dorsolateral prefrontal cortex damage. *J Neuropsychiatry Clin Neurosci* 2016;28:292–298.
- Kaiser RH, Andrews-Hanna JR, Wager TD, Pizzagalli DA. Large-scale network dysfunction in major depressive disorder: a meta-analysis of resting-state functional connectivity meta-analysis of network dysfunction in depression. *JAMA Psychiat* 2015;72:603–611.
- Egorova N, Cumming T, Shirbin C, et al. Lower cognitive control network connectivity in stroke participants with depressive features. *Transl Psychiatry* 2017;7:1–7.
- Pan J, Zhan L, Hu C, et al. Emotion regulation and complex brain networks: association between expressive suppression and efficiency in the Fronto-parietal network and default-mode network. *Front Hum Neurosci* 2018;12:1–12.
- Pascual-Leone A, Rubio B, Pallardó F, Catalá MD. Rapid-rate transcranial magnetic stimulation of left dorsolateral prefrontal cortex in drug-resistant depression. *Lancet* 1996;348:233–237.

38. Fox MD, Liu H, Pascual-Leone A. Identification of reproducible individualized targets for treatment of depression with TMS based on intrinsic connectivity. *Neuroimage* 2013;66:151–160.
39. Michelsen KA, Schmitz C, Steinbusch HWM. The dorsal raphe nucleus—from silver stainings to a role in depression. *Brain Res Rev* 2007;55:329–342.
40. Ikuta T, Matsuo K, Harada K, et al. Disconnectivity between dorsal raphe nucleus and posterior cingulate cortex in later life depression. *Front Aging Neurosci* 2017;9:236.
41. Temel Y, Boothman LJ, Blokland A, et al. Inhibition of 5-HT neuron activity and induction of depressive-like behavior by high-frequency stimulation of the subthalamic nucleus. *Proc Natl Acad Sci U S A* 2007;104:17087–17092.
42. Tan SKH, Janssen MLF, Jahanshahi A, et al. High frequency stimulation of the subthalamic nucleus increases c-fos immunoreactivity in the dorsal raphe nucleus and afferent brain regions. *J Psychiatr Res* 2011;45:1307–1315.
43. Wohlschläger A, Karne H, Jordan D, et al. Spectral dynamics of resting state fMRI within the ventral tegmental area and dorsal raphe nuclei in medication-free major depressive disorder in young adults. *Front Psych* 2018;9:163.
44. Mayberg HS, Starkstein SE, Sadzot B, et al. Selective hypometabolism in the inferior frontal lobe in depressed patients with Parkinson's disease. *Ann Neurol* 1990;28:57–64.
45. Sieger T, Serranová T, Růžicka F, et al. Distinct populations of neurons respond to emotional valence and arousal in the human subthalamic nucleus. *Proc Natl Acad Sci* 2015;112:3116–3121.
46. Herz DM, Zavala BA, Bogacz R, Brown P. Neural correlates of decision thresholds in the human subthalamic nucleus. *Curr Biol* 2016;26:916–920.
47. Péron J, Biseul I, Leray E, et al. Subthalamic nucleus stimulation affects fear and sadness recognition in Parkinson's disease. *Neuropsychology* 2010;24:1–8.
48. Eisenstein SA, Koller JM, Black KD, et al. Functional anatomy of subthalamic nucleus stimulation in Parkinson disease. *Ann Neurol* 2014;76:279–295.
49. Petry-Schmelzer JN, Krause M, Dembek TA, et al. Non-motor outcomes depend on location of neurostimulation in Parkinson's disease. *Brain* 2019;142:3592–3604.
50. Irmén F, Horn A, Meder D, et al. Sensorimotor subthalamic stimulation restores risk-reward trade-off in Parkinson's disease. *Mov Disord* 2019;34:366–376.
51. Grimm S, Beck J, Schuepbach D, et al. Imbalance between left and right dorsolateral prefrontal cortex in major depression is linked to negative emotional judgment: an fMRI study in severe major depressive disorder. *Biol Psychiatry* 2007;63:369–376.
52. Baxter LR Jr, Schwartz JM, Phelps ME, et al. Reduction of prefrontal cortex glucose metabolism common to three types of depression. *Arch Gen Psychiatry* 1989;46:243–250.
53. Husch A, V Petersen M, Gemmar P, et al. PaCER - a fully automated method for electrode trajectory and contact reconstruction in deep brain stimulation. *NeuroImage Clin* 2018;17:80–89.
54. Nowacki A, Nguyen TAK, Tinkhauser G, et al. Accuracy of different three-dimensional subcortical human brain atlases for DBS –lead localisation. *NeuroImage Clin* 2018;20:868–874.
55. Rappel P, Grosberg S, Arkadir D, et al. Theta-alpha oscillations characterize emotional subregion in the human ventral subthalamic nucleus. *Mov Disord* 2020;35:337–343.
56. Al-Fatly B., Ewert S, Kübler D, et al. Connectivity profile of thalamic deep brain stimulation to effectively treat essential tremor. *bioRxiv* 575209 (2019). doi:https://doi.org/10.1101/575209
57. Yao C, Horn A, Li N, et al. Post-operative electrode location and clinical efficacy of subthalamic nucleus deep brain stimulation in Meige syndrome. *Parkinsonism Relat Disord* 2019;58:40–45.
58. Amunts K, Lepage C, Borgeat L, et al. BigBrain: an ultrahigh-resolution 3D human brain model. *Science* (80-. ) 2013;340:1472–1475.